It is therefore to be expected that γ transitions in rather complicated nuclei have more chance of showing an effect. If one is observed in such a nucleus, well and good. However, if no effect is observed, then because of the very complexity of the nucleus, the negative result is difficult to interpret. As pointed out by Wilkinson,[2] the significance of such negative results only increases in proportion to the number of cases investigated. So far only a few experiments have been carried out and it is probably only safe to say that $\mathfrak{F} \leqslant 10^{-4}-10^{-5}$ with any confidence. This is still two orders of magnitude larger than the value of $\mathfrak{F}$ expected from the potential (1).

ACKNOWLEDGMENTS

Comments on various aspects of this work by Professor H. Feshbach, Professor L. Grodzins, Professor T. D. Lee, and Professor V. F. Weisskopf are gratefully acknowledged.

PHYSICAL REVIEW VOLUME 120, NUMBER 1 OCTOBER 1, 1960

Transition Intensities in the Tl^{208} Beta Decay, the $Bi^{212} \rightarrow Po^{212}$ Decay Scheme, and the Bi^{212} Branching Ratio*

G. SCHUPP, H. DANIEL,† G. W. EAKINS, AND E. N. JENSEN
Institute for Atomic Research and Department of Physics, Iowa State University, Ames, Iowa

(Received April 14, 1960)

Studies were made on the Pb^{212} (ThB) active deposit by means of gamma singles and beta-gamma, gamma-gamma, gamma-alpha, and gamma-gamma-alpha coincidence measurements. The singles and coincidence gamma-ray spectra were recorded on an RCL 256-channel analyzer, and an intermediate-image beta-ray spectrometer was used in the beta-gamma work. Beta intensities of 4.6±0.2, 23.9±0.8, 22.7±0.7, 48.8±2.7, and <0.5% were obtained for the 1.04-, 1.29-, 1.52-, 1.80-, and 2.38-Mev groups, respectively, of the $Tl^{208} \rightarrow Pb^{208}$ decay. Existence of the 1.800-Mev gamma ray in Po^{212} was established and 11.2±0.7% of the $Bi^{212} \rightarrow Po^{212}$ disintegrations were determined to go by way of the 0.727-Mev transition. Relative intensities of 11.1±0.7, 1.7±0.3, 0.66±0.07, 0.16±0.04, 0.99±0.08, 0.49±0.05, 2.8±0.2, and 0.17±0.03 were found for the 0.727-, 0.786-, 0.893-, 0.953-, 1.073-, 1.513-, 1.620-, and 1.800-Mev gamma rays, respectively, in Po^{212}. The ratio of alpha to total disintegrations for the Bi^{212} decay was measured to be 0.3596 ±0.0006.

I. INTRODUCTION

THE nuclei Bi^{212} (ThC) and Tl^{208} (ThC″) are members of the naturally radioactive thorium ($4n$) series. Figure 1 shows the generic relations between the last members of this family. Most of the details of the Tl^{208} decay were already known[1–3] before the beginning of the present work while knowledge of the Bi^{212} beta decay was incomplete.[1,4,5]

Reported values for the intensities of the transitions occurring in the beta decay of these nuclei show considerable disagreement. It was the purpose of this investigation to further clarify the scheme of the beta decay of Bi^{212} and to examine the intensities of the radiations resulting from the decay of Tl^{208}. The level schemes of Po^{212} (ThC′) and Pb^{208} (ThD) are interesting because $_{82}Pb_{126}^{208}$ has a doubly magic nucleus and $_{84}Po_{128}^{212}$ has only four nucleons outside the doubly magic core.

The following types of measurements were performed by means of magnetic and scintillation spectrometers: beta- and gamma-ray singles; beta-gamma, gamma-gamma, gamma-alpha, and gamma-gamma-alpha coincidences. The beta-gamma and gamma-gamma coincidences were performed for both decays while the alpha coincidences were used to isolate the Po^{212} gamma rays.

II. EXPERIMENTAL TECHNIQUES

Sources of Pb^{212} (ThB) in equilibrium with its decay products were used in all of the measurements. The magnetic beta-ray spectrometer sources were collected on Al foil of 1.8 mg/cm² and 1-mm diameter whereas those used for the scintillation spectrometers were collected on Pt foil of 50 mg/cm² and 5-mm diameter.

Figure 2 shows the experimental arrangement for the beta-gamma coincidence measurements. The magnetic spectrometer is of the Slätis-Siegbahn type modified[6]

* Contribution No. 871. Work was performed in the Ames Laboratory of the U. S. Atomic Energy Commission.

† On leave from Max Planck Institute for Nuclear Physics, Heidelberg, Germany.

[1] H. Daniel, Ergeb. exakt. Naturw. **32**, 118 (1959). Reviews older work.

[2] E. M. Krisiuk, A. G. Sergeev, G. D. Latyshev, K. I. Il'in, and V. I. Fadeev, J. Exptl. Theoret. Phys. (U.S.S.R.) **33**, 1144 (1958) [translation: Soviet Phys.—JETP **6**, 880 (1958)].

[3] *Nuclear Data Sheets*, edited by C. L. McGinnis (National Academy of Science, Washington, D. C., 1958).

[4] A. G. Sergeev, E. M. Krisiuk, G. D. Latyshev, Yu. N. Trofimov, and A. S. Remmennyĭ, J. Exptl. Theoret. Phys. (U.S.S.R.) **33**, 1140 (1958) [translation: Soviet Phys.—JETP **6**, 878 (1958)].

[5] J. Burde and B. Rozner, Phys. Rev. **107**, 531 (1957).

[6] To be described in a later publication.

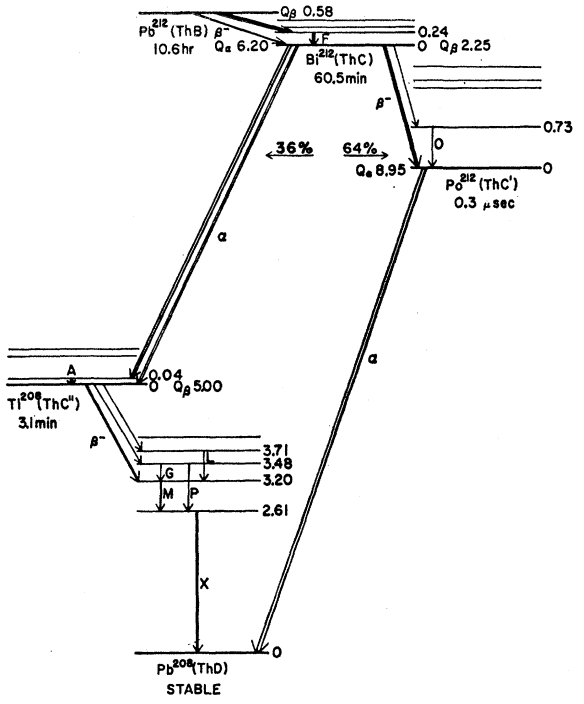

FIG. 1. Disintegration scheme of Pb^{212} and its decay products. Only the more intense transitions are shown. Energies are in Mev.

for electron-gamma coincidence work and for putting two instruments of this kind "back to back" to measure electron-electron coincidences. An anthracene crystal 14 mm in diameter, 1.2-mm thick, and covered with a 150-μg/cm^2 Al film was used as the electron detector. This crystal was coupled to an RCA 6810 photomultiplier by means of a Lucite light pipe with a total reflecting head.[7] The phototube was kept at -55°C by means of a refrigerator unit, and the trigger bias was set low enough to make detection efficiency corrections unnecessary. A Harshaw 3×3 inch NaI(Tl) crystal and Du Mont 6363 photomultiplier were used for the gamma detector. Pb shielding was used to reduce the number of gamma rays backscattered from the end plate into the crystal. A 0.42-g/cm^2 Ta foil was put in front of the crystal to critically absorb the Pb x rays. The pulses from the total gamma-ray spectrum were fed into an RCL 256-channel analyzer which was gated by the coincidence pulses between the gamma rays and whatever energy electrons the spectrometer was set to focus. A discussion of the coincidence circuitry will be deferred until the latter part of this section. Figure 3 shows the singles beta-ray spectrum of Pb^{212} and its decay products as obtained with the magnetic spectrometer at 4% resolution. The arrows indicate settings where coincidence data were taken.

For the gamma-gamma coincidences two Harshaw 3×3 inch NaI(Tl) crystals on Du Mont 6363 photomultipliers were used in 90° positions. The distance between the source and the crystal can in each case was 5.5 cm. A Pb shield 1.5-cm thick was placed between the crystals to eliminate coincidences caused by scattered gamma rays, and a Cu shield of 1.34 g/cm^2 was placed immediately in front of one of the crystals to absorb the beta rays. The Pt source foil was mounted on Al of 0.69 g/cm^2 in such a way as to absorb the beta rays directed toward the crystal without the Cu shield. Coincidence spectra were recorded with the 256-channel analyzer.

In the gamma-alpha coincidence measurements the gamma-ray detection and source mounting were the same as for the gamma-gamma work. The source was placed 2 mm in front of the alpha detector which was a Pilot *B* plastic scintillator 0.45-mm thick and 1 inch in diameter coupled directly to a Du Mont 6292 photomultiplier. This detector resolved the main alpha-ray groups of 6 and 9 Mev shown in Fig. 1 but did not completely separate them from the continuous pulse-height distribution caused by the beta rays. An integral discrimination, with a single-channel analyzer, was made just below the higher-energy alpha-ray peak and these pulses were taken in coincidence with the gamma-ray spectrum which was delayed 0.5 μsec with respect to the prompt coincidence region. Since the coincidence circuit had a $2\tau=0.2$ μsec, the 0.3-μsec half-life of Po^{212} then permitted true gamma-alpha coincidences to be

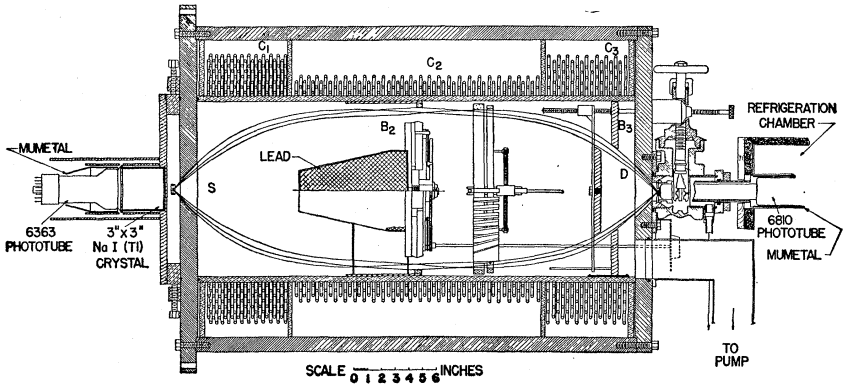

FIG. 2. Schematic drawing of intermediate-image beta-ray spectrometer showing geometry of gamma crystal for beta-gamma coincidence measurements.

[7] P. A. Tove, Rev. Sci. Instr. **27**, 143 (1956).

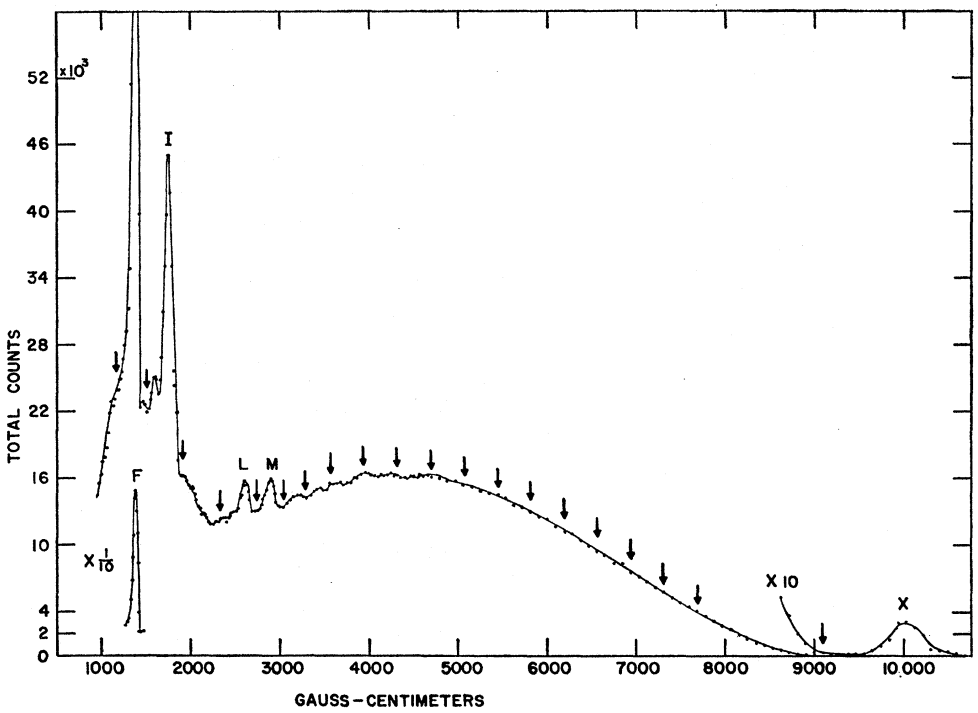

FIG. 3. Beta-ray spectrum resulting from decay of Pb^{212} in equilibrium with its decay products. The arrows indicate settings for beta-gamma coincidence runs.

recorded for an alpha ray detected between 0.4 and 0.6 μsec later than the gamma quantum. Two different geometries were chosen for the gamma crystal; the source-crystal distances were 2.4 cm and 10.6 cm with the source being on the crystal axis in each case.

The same source-crystal arrangement as described in the gamma-gamma work along with the same source-alpha detector geometry discussed above was used for the gamma-gamma-alpha triple coincidence measurements. In this experiment prompt gamma-gamma coincidences were delayed 0.5 μsec with respect to the alpha channel in the manner described above.

Figure 4 shows the geometrical arrangement of the detectors for the triple coincidence work and the block diagram of the electronic circuits used in this investigation. Perhaps the only unusual features of the circuit are the time-jitter adapters[8] which reduce the time jitter in the output of the single-channel analyzers by a factor of approximately six. Blocking oscillator triggers feed the coincidence tubes whereas the coincidence outputs (except C_{12}) go into ordinary univibrator triggers, the bias levels of which adjust the resolving times of the coincidence circuits. These trigger pulses give the various scaler outputs indicated and the triple coincidence output pulse gates the slow coincidence circuit provided in the 256-channel analyzer. The appropriate gating pulses were used in the other coincidence measurements. In all of the experiments Channel 1 was the total gamma-ray spectrum channel, which fed the multichannel analyzer, and Channel 3 was the alpha-ray channel. Channel 2 was the differential gamma-ray channel in the gamma-gamma and gamma-gamma-alpha coincidence measurements, and would properly represent the beta channel in the beta-gamma coincidence work if the amplifier and single-channel analyzer were replaced by a univibrator trigger. In this latter case positive pulses from the 14th dynode of the RCA 6810 photomultiplier were fed into the cathode follower. The single-channel analyzers in Channels 1 and 3 used integral discrimination levels above the x ray and lower-energy alpha-ray group regions, respectively, thereby requiring time-jitter adapters in order that a $2\tau=0.2$ μsec could be used with confidence. No time-jitter adapter was needed in Channel 2 for any of the experiments because of the differential mode of operation for the single-channel analyzer in one case and the fast-rising anthracene pulses in the other. The discrimination level in Channel 1 was chosen to eliminate unnecessary accidental coincidences and exhibits itself in the coincidence spectra as a low-energy cutoff.

For evaluation of the data, each coincidence gamma-ray spectrum was first corrected point by point for accidental coincidences. This correction was made by normalizing the associated singles gamma spectrum to give the total number of accidentals calculated from the measured resolving time, the total number of gamma and beta singles counts, and the Pb^{212} half-life. The

[8] G. W. Eakins, B. J. Loupee, W. A. Rhinehart, G. Schupp, and E. N. Jensen, Ames Laboratory Report ISC-804, 1956 (unpublished).

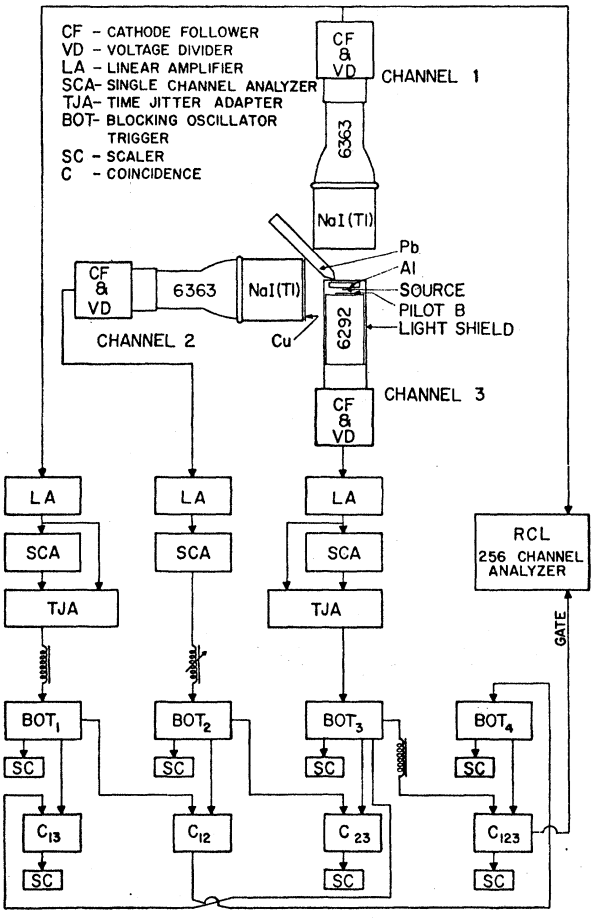

FIG. 4. Geometrical arrangement of detectors and block diagram of the associated electronic circuitry used in gamma-gamma-alpha coincidence experiment.

average length run was about 4 hours. The resulting spectrum of true coincidences was separated into its various photopeak and Compton distributions by subsequent subtractions. The resolution of each peak was obtained from the measured values of the resolution for the 0.662-Mev Cs^{137} gamma ray and the 2.614-Mev X line of the Tl^{208} decay. The peak-to-total ratio for each gamma ray was deduced from the experimental curve of Heath,[9] fitted to the measured values for the 0.662- and 2.614-Mev gamma rays. Figure 5 shows the singles gamma-ray spectrum resulting from the Pb^{212} decay resolved into its different gamma-ray components. The low-energy part of the spectrum was studied at a higher amplifier gain setting. A source-crystal distance of 23 cm with the Cu shield of 1.34 g/cm² in front of the Harshaw 3×3 inch NaI(Tl) crystal was used in the study of the singles spectrum. In order to obtain the beta-ray spectrum in coincidence with a particular gamma ray (photopeak plus Compton distribution), the first step was to determine the percentage of that particular gamma ray in the coincidence spectrum to the total coincidence gamma-ray spectrum for each of the beta-gamma coincidence runs. The relative source strengths were determined by recording the initial beta counting rate at 4743 gauss-cm. The different length coincidence runs were normalized by calculating, from the total coincidence counts, the initial coincidence counting rate of each run. The normalized coincidence counting rates with a particular gamma ray were then plotted as a function of the beta-ray momentum. In some cases the percentage attributed to a particular gamma ray included part of another gamma ray of nearly equal energy. For these cases, corrections were made later in the analysis of the components of the coincidence beta-ray spectra.

[9] R. L. Heath, Idaho Operations Office Report IDO-16408, 1957 (unpublished).

III. RESULTS

Figure 6 shows, as an example, the gamma-ray spectrum in coincidence with 1.106-Mev beta rays. The amount of annihilation radiation, resulting from the 2.614-Mev gamma ray, contained in the 0.511-Mev peak was estimated from coincidence spectra in which the 0.511-Mev gamma ray was not in coincidence with the observed beta rays. Gain shifts during the individual runs invariably broadened the 2.614-Mev gamma-ray photopeak disproportionately with respect to the lower energy components of the spectrum because of its much higher energy and associated smaller resolution. The resulting high relative intensity of the beta-ray spectrum in coincidence with the 2.614-Mev gamma ray was then normalized to the sum of the relative intensities of the beta groups leading to the 2.614-Mev level in Pb^{208}, as determined from coincidences with the other gamma rays. It was possible to make this normalization because the intensity of the beta group going directly to that level was measured to have an upper limit of 0.5% of the Tl^{208} beta transitions.

The experimental beta-ray spectrum from Bi^{212} in

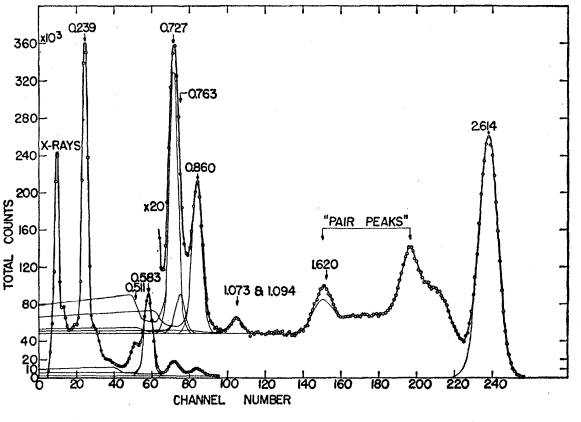

FIG. 5. Gamma-ray spectrum of Pb^{212} in equilibrium with its decay products. The fine lines show the estimated photopeak and Compton distributions. Energies are in Mev.

TABLE I. Summary of results.

Gamma-ray energy Mev	Rel. No. of β-γ coincidences[a] "unchecked"		Rel. No. of β-γ coincidences[a] "checked"		Rel. gamma-ray intensities from singles and γ-γ coincidences	Transition intensities %
			$Tl^{208} \rightarrow Pb^{208}$			
	33.2	β_1	4.6±0.2	β_1		
		β_2	22.5±1.1	β_2		
2.614	18.4	β_3	23.0±1.2	β_3	9.5 ±0.5	(100)
	48.4	β_4	49.9±3.5	β_4		
	Total 100.0					
1.094	0.9±0.1	β_1	0.04	β_1	0.06±0.01	0.7 ±0.1
		β_2	0.9±0.1	β_2		
		β_1	0.06	β_1		
0.860	14.9±0.7	β_2	0.2±0.1	β_2	1.20±0.06	14.2 ±0.6
		β_3	14.6±0.7	β_3		
0.763	...		...		0.29±0.02	3.4 ±0.2
	22.2	β_1	4.5±0.2	β_1		
		β_2	21.4±1.1	β_2		
0.583	15.5	β_3	8.4±0.5	β_3	7.25±0.35	85.1 ±4.0
	46.5	β_4	49.9±3.5	β_4		
	Total 84.2±3.3					
	3.0	β_1	1.1±0.1	β_1		
0.511	19.4	β_2	21.3±1.1	β_2	2.01±0.10	25.3 ±1.2
	Total 22.4±0.8					
0.486	...		...		0.01±0.01	0.1 ±0.1
0.277	...		...		...	8.6[b]
0.253	...		...		...	1.1[b]
0.233	...		...		...	0.3[b]
			$Bi^{212} \rightarrow Po^{212}$			[c]
1.800	...		...		...	0.18±0.03
1.620	4.7±0.2	β_3	4.7±0.2	β_3	0.23±0.03	2.82±0.20
1.513	...		...		...	0.50±0.05
1.073	1.2±0.3	β_1	1.2±0.3	β_1	0.10±0.02	1.00±0.08
0.953	...		...		...	0.17±0.04
0.893	...		...		...	0.67±0.07
0.786	...		...		...	1.75±0.27
		β_1	1.2±0.3	β_1		
	7.4	β_2	0.3±0.1	β_2		
0.727		β_3	1.1±0.1	β_3	1.65±0.08	11.2 ±0.7
		β_4	3.4±0.5	β_4		
	14.5±1.0	β_5	15.8±0.9	β_5		
	Total 21.9±0.6					

[a] The total number of betas in coincidence with the 2.614-Mev transition as well as with the sum of the 1.094-, 0.860-, and 0.583-Mev transitions were normalized to 100. Thus all the β-γ coincidence numbers associated with the $Tl^{208} \rightarrow Pb^{208}$ decay correspond to the actual percentage of Tl^{208} disintegrations going by way of both the beta group indicated and the transition whose gamma-ray energy is shown in Column 1. The number of β-γ coincidences in the $Bi^{212} \rightarrow Po^{212}$ decay are kept relative to the beta coincidence numbers in the $Tl^{208} \rightarrow Pb^{208}$ decay and therefore are not transition percentages. "Checked" and "unchecked" refer to whether or not the numbers were checked for internal consistency.
[b] Values obtained from ratios with respect to 0.583-Mev transition as given by Krisiuk *et al.*[2]
[c] Values obtained from alpha-gamma coincidence data normalizing to 11.2% for the 0.727-Mev transition (see Sec. III).

coincidence with the 0.727-Mev gamma ray is shown by the circles in Fig. 7. The Fermi analysis of this spectrum, which was done independently of any known energy values, decay schemes, etc., gave the beta components shown in the figure. In most cases, however, particularly for the complicated coincidence spectra in the Tl^{208} decay, the end points were assumed in order to give the best relative intensities for the subsequent subtractions. An allowed shape factor was used for all the beta spectra. This is in agreement with the spin and parity assignments (see Sec. IV). The results of the beta-gamma coincidence measurements unchecked for internal consistency, except for the renormalization of the total spectrum in coincidence with the 2.614-Mev gamma ray mentioned earlier, are given separately for the Tl^{208} and Bi^{212} decays in the second column of Table I. The "checked" values in Table I were obtained from the total number of beta rays in coincidence with each gamma ray, incorporating gamma-ray intensities and branching ratios where necessary. Summing, ab-

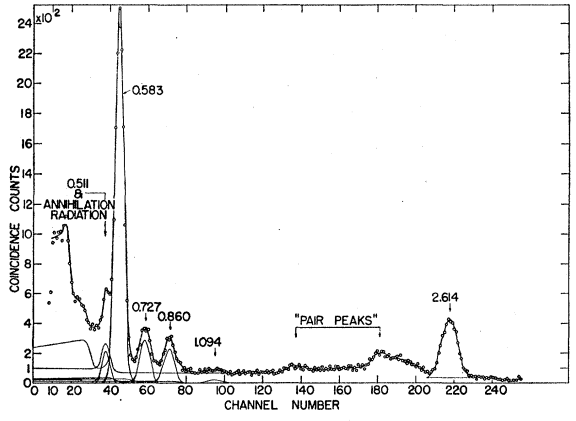

FIG. 6. Gamma-ray spectrum in coincidence with 1.106-Mev beta rays. Energies are in Mev.

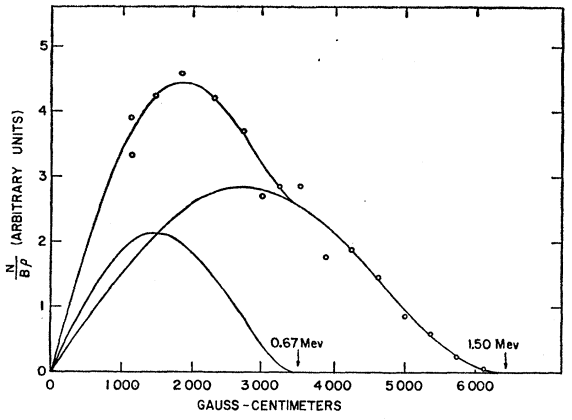

FIG. 7. Beta-ray spectrum in coincidence with the 0.727-Mev gamma ray. The arbitrary scale unit results from N being a normalized coincidence counting rate.

sorption, and internal conversion corrections have been applied.

Gamma-ray spectra were taken in coincidence with gamma rays having energies of 2.614, 0.860, and 0.727 Mev. The first two are gamma rays in Pb^{208} and the third one is a gamma ray in Po^{212}. Figure 8 shows the gamma-ray spectrum found in coincidence with the 2.614-Mev gamma ray. Summing corrections showed that 0.4 of the highest-energy peak was due to the 1.094-Mev gamma ray. The gamma-ray spectrum in coincidence with the 0.727-Mev gamma-ray photopeak region is given in Fig. 9. The difference between these two

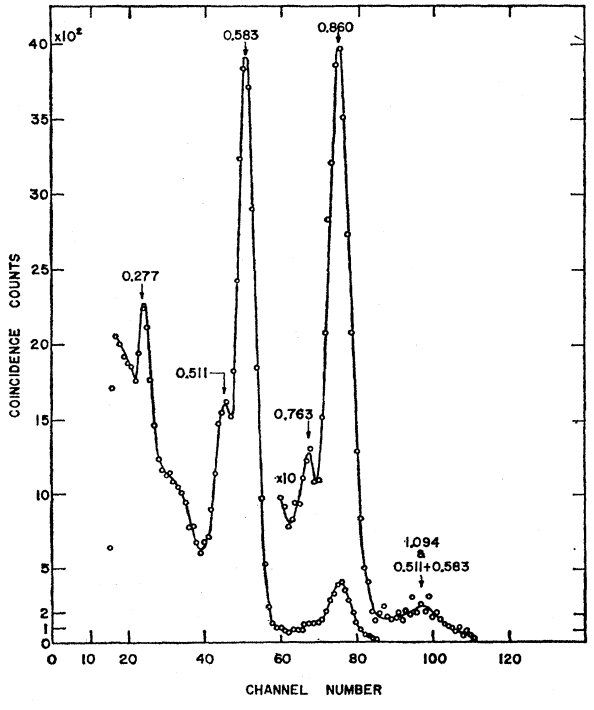

FIG. 8. Gamma-ray spectrum in coincidence with the 2.614-Mev gamma ray. Energies are in Mev.

curves, normalized such that there would be no 0.583-Mev gamma-ray peak, is shown in Fig. 10(A). This difference spectrum eliminates the unwanted coincidences, caused by Comptons from the 2.614-Mev gamma ray in the 0.727-Mev region, and essentially gives the gamma spectrum in coincidence with the 0.727-Mev gamma ray. The 0.727-Mev gamma ray itself appears in this spectrum because of the Compton and photopeak distributions from gamma rays actually in coincidence with it which were in the 0.727-Mev region of the differential analyzer. The continuous distribution shown in this spectrum is due to the Comptons of the 2.614-Mev gamma ray in coincidence with the 0.763-Mev gamma ray which was also in the 0.727-Mev region. Irregularities around 0.583 Mev were caused by a slight gain shift and accentuated by the differences between large numbers. A similar subtraction of the low-energy gamma-ray spectrum in coincidence with the 2.614-Mev gamma ray from the low-energy gamma-ray spectrum in coincidence with the 0.860-Mev region, normalized

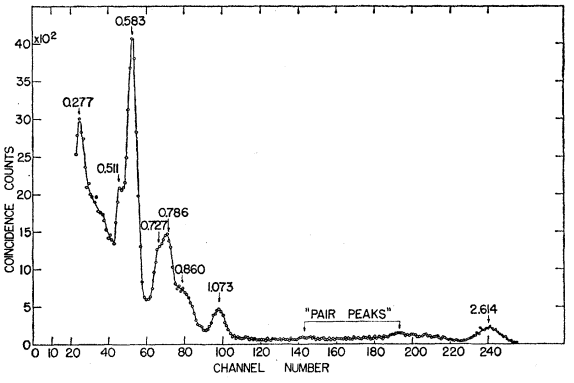

FIG. 9. Gamma-ray spectrum in coincidence with photopeak region of the 0.727-Mev gamma ray. Energies are in Mev.

to give no 0.583-Mev peak, gave an upper limit of 1/50 of the 0.511-Mev gamma-ray intensity for the intensity of the 0.486-Mev gamma ray. From these data the best estimate for the above intensity ratio is 1/200.

The gamma-ray spectrum in delayed coincidence with the 9-Mev alpha-ray group is shown in Fig. 11. This spectrum was run at the 10.6-cm source-crystal distance and the combination of these data with the 2.4-cm geometry data gave good estimates for the gamma-gamma pulse-height summing and, after absorption corrections, the relative gamma-ray intensities listed in Table III (see Sec. IV). Special care was taken in establishing the existence of the 1.800-Mev gamma ray because of its importance in the level scheme (see Sec. IV). The summing correction at the 10.6-cm distance was 14% for the 1.800-Mev photopeak.

Figure 10(B) shows the results of the gamma-gamma-alpha triple coincidence measurements. These data were obtained by having the gamma-ray spectrum in prompt coincidence with the 0.727-Mev region, and both in

delayed coincidence with the 9-Mev alpha-ray group. Thus both curves of Fig. 10, although obtained differently, show the same spectrum of gamma rays in coincidence with the 0.727-Mev region of the gamma-ray spectrum associated with the Bi^{212} beta decay.

Analysis of the singles gamma-ray spectrum shown in Fig. 5 employed the ratio of the 0.860- and 0.763-Mev photopeaks as obtained from Fig. 8. The curve given by Heath[9] for the gamma-ray spectrum of Na^{24}, which has a 2.76-Mev gamma ray, was used to estimate the height of the second escape peak from the 2.614-Mev gamma ray. This last comparison indicated good agreement between Heath's gamma-ray spectra and those of this investigation, thus giving further justification for the peak-to-total ratios used throughout in the evaluation of these data. The ratios of the photopeaks of the 0.239- and 0.511-Mev gamma rays to that of the 0.583-Mev

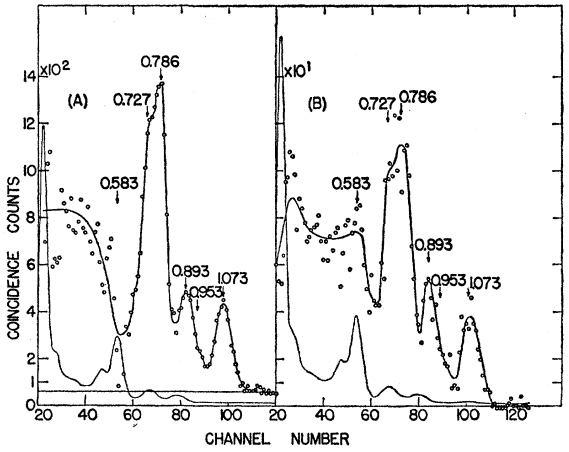

FIG. 10. (A) Gamma-ray spectrum in coincidence with the photopeak region of the 0.727-Mev gamma ray normalized to exclude coincidences with Comptons from the 2.614-Mev gamma ray. (B) Po^{212} gamma-ray spectrum in prompt coincidence with the 0.727-Mev region and in delayed coincidence with the 9-Mev alpha-ray group. The corresponding singles spectra for both (A) and (B) are shown for energy comparison. Energies are in Mev.

gamma ray were taken from the spectrum run at the higher gain setting. Relative transition intensities for the two decay schemes are given in Table I.

The relative intensities of the 0.239 (F line)-, 0.583-, 0.727-, 0.860-, 1.094-, and 2.614-Mev transitions, as determined from the gamma-ray singles analysis, were used to determine the fraction of the Bi^{212} beta decays going by way of the 0.727-Mev transition. A value of 0.121 ± 0.012 was obtained by way of the 0.239-Mev F-line gamma ray in the Pb^{212} decay, using a total internal conversion coefficient of 0.81[10–11] and an intensity of 74%[11] for the F-line transition, a decay equilibrium

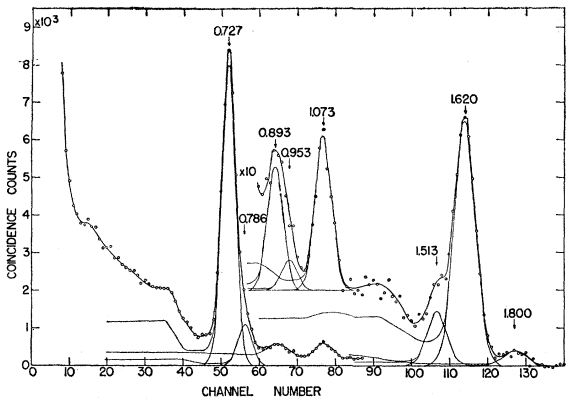

FIG. 11. Gamma-ray spectrum in delayed coincidence with the Po^{212} alpha rays. Energies are in Mev.

correction factor of 1.105, and 64.04% for the beta branching of the Bi^{212} decay. Using the same alpha-beta branching ratio and 100% for the 2.614-Mev transition in the Tl^{208} decay, the value calculated was 0.099 ± 0.007. Taking the sum of the intensities of the 0.583-, 0.860-, and 1.094-Mev transitions as 100% gave a value of 0.108 ± 0.007. By way of the sum of the relative number of beta rays in coincidence with the 0.583-, 0.860-, and 1.094-Mev transitions to those in coincidence with the 0.727-Mev transition as found in the beta-gamma coincidence measurements, using the same normalization as above, a value of 0.123 ± 0.006 was obtained. A decay equilibrium correction factor of 1.005 was used for these last three determinations. An average value of 0.112 ± 0.007 was taken for the 0.727-Mev transition.

The value for the branching of the Bi^{212} decay was obtained from the intensities of the 6- and 9-Mev alpha-ray groups of the Bi^{212} and Po^{212} decays, respectively. The alpha detector was a Harshaw-prepared CsI(Tl) crystal, 3 mil thick and 1.5-inch diameter, acquired during the final stages of this investigation. A piece of 25-mil brass with a $\frac{1}{8}$-inch diameter collimating orifice was placed in front of the crystal to minimize the path lengths in the scintillator for the beta rays. A typical alpha-ray spectrum is shown in Fig. 12. A total of eleven

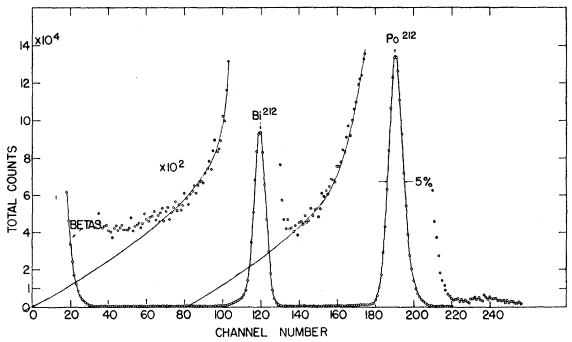

FIG. 12. A typical alpha-ray spectrum resulting from the decay of Pb^{212} and its decay products as obtained with a 0.003-inch thick CsI(Tl) crystal.

[10] E. M. Krisiuk, G. D. Latyshev, M. A. Listengarten, L. A. Ostretsov, and A. G. Sergeev, Izvest. Akad. Nauk S.S.S.R. Ser. Fiz. **20**, 363 (1956) [translation: Bull. Acad. Sciences U.S.S.R. **20**, 332 (1956)].

[11] E. M. Krisiuk, A. G. Sergeev, G. D. Latyshev, and V. D. Vorob'ev, Nuclear Phys. **4**, 579 (1957).

TABLE II. Comparison of Tl^{208} beta-group intensities.

Beta group	End-point energy Mev	Percent of Tl^{208} decays This investigation β-γ coinc. data	γ-ray rel. int.	Av.	Log *ft*	Nuclear data sheets[a]	Krisiuk *et al.*[b]
β_1	1.04	4.6±0.2	4.6±0.2	4.6±0.2	5.8	4	4
β_2	1.29	22.5±1.1	25.2±1.2	23.9±0.8	5.3	33	23
β_3	1.52	23.0±1.2	22.4±0.8	22.7±0.7	5.7	16	20
β_4	1.80	49.9±3.5	47.8±4.2	48.8±2.7	5.7	47	52
β_5	2.38	<0.5	···	<0.5	>8.1	≈0.03	1.5

[a] See reference 3.
[b] See reference 2.

runs were made with different source intensities and source-crystal distances. The results showed no correlation with intensity or geometry and were averaged to give a value of 0.3596±0.0006 for the alpha branching of Bi^{212}. The error assignment estimated from deviations about the mean was 0.0004, whereas the error expected from the total number of counts involved was only 0.0002. This difference reflects the dependence of the value upon the manner in which the tails were drawn for the two alpha-ray peaks. The calculated standard deviation of 0.0004 was increased to 0.0006 to allow for a possible systematic error in the extrapolation of the tails.

The CsI(Tl) crystal, with orifice, was used to check the alpha-gamma coincidence work done earlier in this investigation using the Pilot *B* scintillator. In this case no concern had to be given to beta-gamma coincidences since the alpha- and beta-ray pulse heights were completely separated as shown in Fig. 12. The results were in agreement with the earlier Pilot *B* data and the existence of the 1.800-Mev gamma-ray was further established by runs taken with a source-crystal distance of 15 cm.

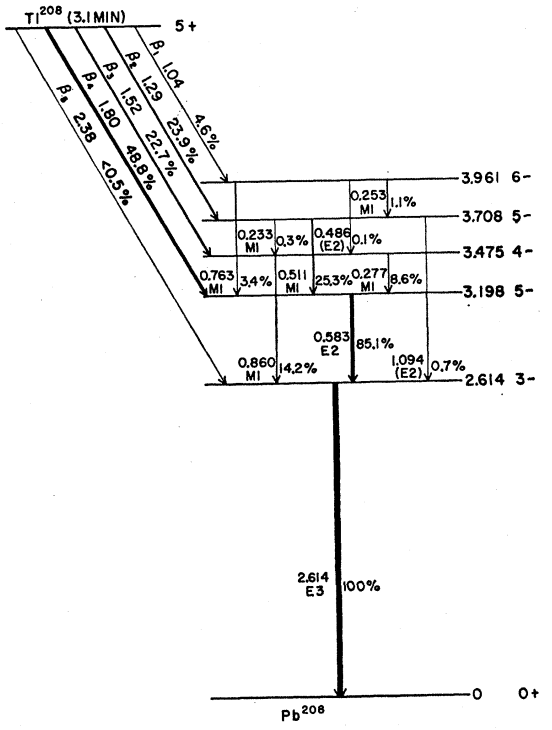

FIG. 13. Decay scheme of Tl^{208}. Energies are in Mev.

IV. DISCUSSION

$Tl^{208} \rightarrow Pb^{208}$

The decay scheme resulting from the beta decay of Tl^{208} is shown in Fig. 13. The intensities given are those measured in the present investigation with the exception of the 0.277-, 0.253-, and 0.233-Mev transitions which were taken from intensity ratios with respect to the 0.583-Mev transition as given by Krisiuk *et al.*[2] This same reference was used in making the level assignments. The beta-group percentages were determined both from the beta-gamma coincidence data and from the intensities of the gamma-ray transitions corrected for internal conversion. In the latter case the sum of the 0.583-, 0.860-, and 1.094-Mev transitions was normalized to 100%. The average values were obtained and are shown in Fig. 13.

A comparison between beta-group percentages as obtained in this investigation and previously published percentages is shown in Table II. The log *ft* values of the nonunique first-forbidden beta groups are comparatively low, a fact in line with observations on several other nuclei in this region.[1]

$Bi^{212} \rightarrow Po^{212}$

From the results given in Sec. III, a decay scheme for the beta decay of Bi^{212} can be constructed which is internally consistent with all the data of this investigation. In addition, results are incorporated from other work on quantities not measured in the present investigation, e.g., alpha-ray energies and intensities.[12] Figure 14 shows the decay scheme obtained in this way.

The average value of 11.2% for the intensity of the 0.727-Mev transition served as the normalization for assigning all other transition percentages. The beta-group intensities were derived from the gamma-ray transition intensities, but in the few cases where beta-gamma coincidence data could be used the agreement

[12] G. H. Briggs, Revs. Modern Phys. **26**, 1 (1954).

was good. The partial half-lives of the Bi^{212} beta-decay components gave log ft values of 7 ± 1 for all the beta groups, which is characteristic for first-forbidden non-unique transitions. Since Bi^{212} has a ground-state assignment of 1-,[13] all levels in Po^{212} must be 0+, 1+, or 2+. Alpha-ray selection rules[14] preclude alpha decay from a 1+ level to the ground-state 0+ level of Pb^{208}. Therefore, all alpha-emitting levels in Po^{212} must be either 0+ or 2+. Since the Po^{212} ground state is 0+ (even-even nucleus), the 0.727- and 1.800-Mev alpha-emitting levels must be 2+ because they also decay by gamma emission to the ground state. The assignment of $E2$ to the 0.727- and 1.800-Mev transitions is thus to be expected. The gamma-ray and alpha-ray relative intensities from the 0.727- and 1.800-Mev levels are also consistent with what would be predicted using the partial half-lives of the alpha decay[15] and the half-life for $E2$ transitions.[16]

The assignments of 2+ and 1+ to the 1.513- and 1.620-Mev levels, respectively, are made on the basis of the relative intensities of the transitions leaving these levels. The ratio of the 0.786- to the 1.513-Mev transition is consistent with the former being $M1$ and the latter pure $E2$. This ratio is also approximately the same as the ratio of the 1.073- to the 1.800-Mev transition. The ratio of the 0.893- to the 1.620-Mev transition is consistent with both of them being the same multipolarity, namely $M1$. Internal conversion coefficients were calculated from the gamma-ray intensities obtained in this investigation and the conversion-electron intensities given by Sergeev *et al.*[4] The multipolarity assignments determined from these calculated conversion coefficients and the internal conversion tables of

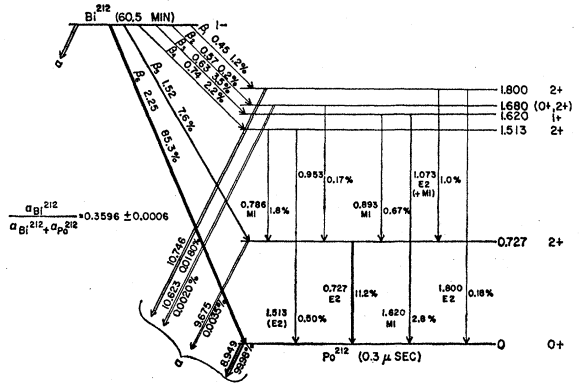

FIG. 14. $Bi^{212} \rightarrow Po^{212}$ decay scheme. The alpha-ray energies include the recoil energies of the Pb^{208} nuclei. Energies are in Mev.

TABLE III. Multipolarity assignments for the electromagnetic transitions in Po^{212}. Intensities are in percent of $Bi^{212} \rightarrow Po^{212}$ transitions and α_K is the internal conversion coefficient in the K-shell.

Transition energy (Mev)	I_γ (%)	I_{eK} (%)[a]	α_K (exp)	α_K (theo)[b]	Assignment
0.727	11.1 ±0.7	0.106	0.0095 ±0.0011	0.0105 ($E2$)	$E2$
0.786	1.70 ±0.26	0.051	0.030 ±0.005	0.032 ($M1$)	$M1$
0.893	0.66 ±0.07	0.014	0.021 ±0.003	0.023 ($M1$)	$M1$
0.953	0.16 ±0.04	0.010	0.063 ±0.015	0.046 ($M2$)	···
1.073	0.99 ±0.08	0.006	0.006 ±0.001	0.014 ($M1$)	$E2$
				0.0052 ($E2$)	($+M1$)
1.513	0.49 ±0.05	0.008	0.016 ±0.002	0.0027 ($E2$)	($E2$)
1.620	2.81 ±0.20	0.013	0.0046 ±0.0006	0.0050 ($M1$)	$M1$
1.800	0.17 ±0.03	0.007	0.041 ±0.007	0.002 ($E2$)	$E2$

[a] Intensities of the internal conversion electrons are those given by Sergeev *et al.*[4]
[b] From internal conversion tables of Sliv and Band.[17]

Sliv and Band[17] are in agreement with those given above. Exceptions to this statement are the 1.513- and 1.800-Mev transitions which, on the basis of transition probabilities and almost certain level assignments, must be $E2$, but both have a large excess of internal conversion electrons as shown in Table III.

The absence of observed alpha decay from the 1.513- and 1.620-Mev levels can be explained in the latter case by the 1+ assignment and in the former case only on the basis of an expected low alpha-ray intensity. Comparing intensities and partial half-lives of the gamma- and alpha-ray transitions from the 1.513- and 0.727-Mev levels would indicate an expected intensity on the order of one alpha decay from the 1.513-Mev level for every 35 alpha decays from the 0.727-Mev level.

The 1.680-Mev level can be either 0+ or 2+ since this level emits alpha radiation. No gamma-ray cross-over transition to the 0+ ground state has been detected which would support the assignment of 0+ for the 1.680 level. However, the 1.680-Mev gamma ray may be present and its intensity too low to be detected in this investigation so that a 2+ assignment cannot be ruled out. Assuming the same ratio for the 1.680- to the 0.953-Mev transition as for the 1.800- to the 1.073-Mev transition, the 1.680-Mev transition, if it were present, would be approximately $\frac{1}{5}$ the intensity of the 0.953-Mev transition which itself is quite weak.

There is the question of how to describe a nucleus like Po^{212} with four nucleons outside the doubly-magic core. Shell-model calculations with the interaction between the outside nucleons being taken into account are not available though it would be very interesting to compare theory and experiment in this case. On the other hand, collective phenomena may be of some importance. The experimental evidence, however, indicates otherwise since the vibrational model[18–19] would predict the transi-

[13] J. W. Horton, Phys. Rev. **101**, 717 (1956).
[14] J. M. Blatt and V. F. Weisskopf, *Theoretical Nuclear Physics* (John Wiley & Sons, New York, 1952), p. 571.
[15] I. Perlman and J. O. Rasmussen, *Encyclopedia of Physics* (Springer-Verlag, Berlin, 1957), Vol. 42, p. 141.
[16] S. A. Moszkowski, in *Beta- and Gamma-Ray Spectroscopy*, edited by K. Siegbahn (Interscience Publishers, Inc., New York, 1955), p. 391.
[17] L. A. Sliv and I. M. Band, Leningrad Physico-Technical Institute Report, 1956 [translation: Report 57ICC K1, issued by Physics Department, University of Illinois, Urbana, Illinois (unpublished)].
[18] G. Scharff-Goldhaber and J. Weneser, Phys. Rev. **98**, 212 (1955).
[19] L. Wilets and M. Jean, Phys. Rev. **102**, 788 (1956).

tion from the second 2+ level to the first 2+ level to be mainly $E2$, whereas the experimental finding is $M1$. It should be kept in mind that the vibrational model was proposed mainly for other regions of the periodic system.

The results of this investigation are in essential agreement with the decay schemes presented by Krisiuk *et al.*,[2] Sergeev *et al.*,[4] Emery and Kane,[20] and Hauser and Kerler.[21] The observation of a 1.800-Mev gamma ray in Po^{212} and hence the 2+ assignment for the 1.800-Mev level, however, is in disagreement with the 0+ assignment of Emery and Kane[20] and Martin and Parry.[22]

The 0.3596 ± 0.0006, $\alpha/(\alpha+\beta)$ branching ratio of Bi^{212} determined in this investigation is somewhat larger than the 0.354 ± 0.004 value[23] used by Emery and Kane.[20] It is in good agreement only with the 0.362 ± 0.006 value reported by Senftle *et al.*[24] and is larger than all other values reported, beginning with the original determination by Marsden and Barratt[25] and including the work by Prosperi and Sciuti.[26]

ACKNOWLEDGMENTS

Thanks are due to Dr. B. C. Carlson for helpful theoretical discussions, to Barry McDaniel for his assistance in evaluation of the data, to Emery and Kane,[20] and to Hauser and Kerler[21] for making their results available to us prior to publication.

[20] G. T. Emery and W. R. Kane, Phys. Rev. **118**, 755 (1960).
[21] U. Hauser and W. Kerler, Z. Physik (to be published).
[22] D. G. E. Martin and G. Parry, Proc. Phys. Soc. (London) **A68**, 1177 (1955).
[23] P. Marin, G. R. Bishop, and H. Halban, Proc. Phys. Soc. (London) **A66**, 608 (1953).
[24] F. E. Senftle, T. A. Farley, and N. Lazar, Phys. Rev. **104**, 1629 (1956).
[25] E. Marsden and T. Barratt, Proc. Phys. Soc. (London) **24**, 50 (1911).
[26] D. Prosperi and S. Sciuti, Nuovo cimento **9**, 734 (1958).

PHYSICAL REVIEW VOLUME 120, NUMBER 1 OCTOBER 1, 1960

Angular Distribution of Fragments in Fission Induced by Mev Neutrons

J. E. SIMMONS AND R. L. HENKEL*
Los Alamos Scientific Laboratory, University of California, Los Alamos, New Mexico
(Received April 1, 1960)

A multiangle gas-filled counter has been used to measure the fragment angular distribution in fission induced by neutrons in the energy range $0.5 \leq E_N \leq 9$ Mev. The target nuclei used were: Th^{230}, U^{233}, U^{234}, U^{235}, U^{236}, U^{238}, Np^{237}, and Pu^{239}. In the cases of U^{233} and U^{235} the neutron energy range was extended to include energies between 14.8 and 23 Mev. The general features of these data are the following: The anisotropy—(0°/90°) intensity ratio—has values between 1.1 and 1.2 depending on the target and is roughly independent of energy for E_N between 2 and 5.5 Mev. At higher energies a rise is observed such that at 7 Mev even-odd targets give values of anisotropy in the range 1.2 to 1.3 while even-even targets show greater values in the range 1.6 to 2.2. The anisotropy decreases somewhat by 9 Mev. Near thresholds for the even-even target nuclides considerable fluctuations of anisotropy are observed. The example of U^{236} at 0.85 Mev shows a new case of minimum intensity at 0°, the anisotropy being 0.64. In the energy region 2–4 Mev, the anisotropy of Pu^{239}, U^{233}, and U^{235} increases by a few percent from one to the next as the spin increases. This is contrary to simple theoretical expectations. These data have been compared to recent theoretical developments of the Bohr model as given by Griffin and by Halpern and Strutinski. The theory provides a satisfactory account of many features of the data.

I. INTRODUCTION

THE angular distribution of fragments from nuclear fission is related to the manner in which angular momentum is conserved. Hill and Wheeler[1] set forth a qualitative picture in a first attempt to explain early experiments on photofission[2] and neutron-induced fission.[3] At the 1955 Geneva Conference Bohr[4] presented a detailed model relating angular distributions of the fragments to the existence of rotational quantum states of the highly deformed nucleus at the barrier for fission. Wilets and Chase[5] have used this picture to fit an angular distribution in the fission[6] of Th^{232} induced by neutrons near the threshold. More recently Strutinski,[7] Halpern and Strutinski,[8] and Griffin[9] have presented more detailed developments of the Bohr model applicable when large numbers of quantum states are

* This work was supported by the U. S. Atomic Energy Commission.
[1] D. L. Hill and J. A. Wheeler, Phys. Rev. **89**, 1102 (1953).
[2] E. J. Winhold, P. T. Demos, and I. Halpern, Phys. Rev. **87**, 1139 (1952).
[3] J. E. Brolley, Jr., and W. C. Dickinson, Phys. Rev. **94**, 640 (1954).
[4] A. Bohr, *Proceedings of the International Conference on the Peaceful Uses of Atomic Energy, Geneva, 1955* (United Nations, New York, 1956), Vol. 2, p. 151.
[5] L. Wilets and D. M. Chase, Phys. Rev. **103**, 1296 (1956).
[6] R. L. Henkel and J. E. Brolley, Jr., Phys. Rev. **103**, 1292 (1956).
[7] V. M. Strutinski, Atomnaya Energ. **2**, 508 (1957) [translation: Soviet J. Atomic Energy **2**, 621 (1957)].
[8] I. Halpern and V. M. Strutinski, *Proceedings of the Second United Nations International Conference on the Peaceful Uses of Atomic Energy, Geneva, 1958* (United Nations, Geneva, 1958), Vol. 15, p. 408.
[9] J. J. Griffin, Phys. Rev. **116**, 107 (1959).